THE INFLUENCE OF PROCESS PARAMETERS ON THE DEFORMATION FORCE WHEN ROLLING TRAPEZOIDAL PROFILES WITH RACK TOOLS

Ion UNGUREANU[1], Mădălin TUDOR[1], Eduard NITU[1], Doina IACOMI[1], Monica IORDACHE[1]
[1]University of Pitesti, Romania

ABSTRACT
This paper presents the research made on the modelling of forces when processing profiles corresponding to trapezoidal thread through cold deformation with rack tools. For proper orientation of the experimental research a theoretical study was made on the process and the parameters which influence the force were determined. Three possible models were established for the deformation force and an experience plan to allow determining the established models was performed. A stand with all the adequate means to measure process parameters was designed and built. The data acquired, corresponding to the experience plan established, were processed using LINEST application of EXCEL software. Therefore, there were determined the machinability functions which allow calculating the deformation forces when processing a trapezoidal profile on cylindrical pieces. The way in which process variables influence the size of the deformation force was analysed.

KEYWORDS
cold forming, rolling process, rolling flat wedges, forming force, machinability functions

INTRODUCTION

Processing through cold plastic deformation with rack tools is widely used in mass production and is frequently used to achieve profiles on cylindrical pieces. The procedure is very productive and it ensures high precision, continuous fibre, superior mechanical properties compared to the initial material, and low roughness at the surface of profiles [5]. Processing quality can be compromised if process parameters are not identified and properly managed. Therefore, by exceeding some limits of material stress, cracks, exfoliations of the superficial layer, etc. can appear in the deformed material. To avoid such phenomena, it is required to know the way in which the deformation process takes place and which are the process parameters with the greatest influence on forces, tensions in the deformed material, roughness of the processed surfaces, etc. [1]. In the case of processing some profiles, such as trapezoidal threads, these influences of process parameters on the final results of processing are not very well known. For this reason, the research performed, partially presented in this paper, aims to establish some machinability functions related to the deformation forces, which are then analysed through multiple linear regression methods.

THEORETICAL ASPECTS REGARDING THE MODELLING OF DEFORMATION FORCES

The process of rolling circular profiles, trapezoidal profiles SR ISO 2904:1996, fig. 1, with rack tools consists in using two racks which move in opposite directions fig. 2.

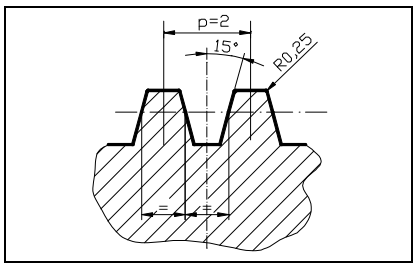

Figure 1. Geometry of processed profiles

To obtain profiles on a cylindrical piece with the initial diameter d_0, the two racks are provided with profiles whose peaks are processed inclined, slope $P = \frac{H}{L} = tg\alpha_0$ [2].

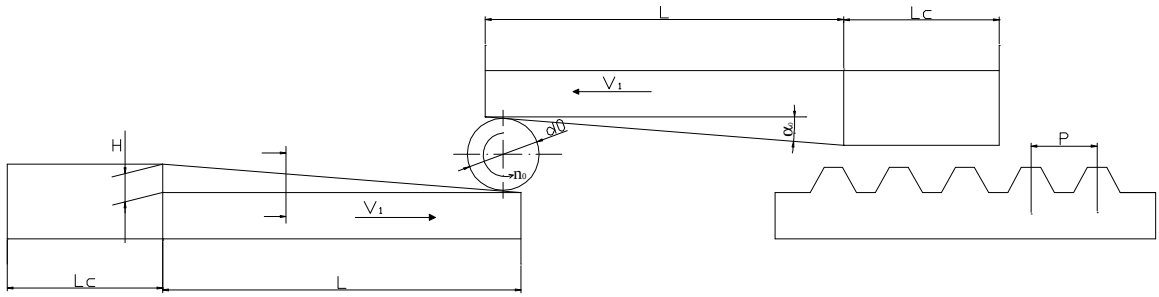

Figure 2. Scheme to generate profiles with rack tools

The constructive form of racks, conical in the working area of length L, provides a gradual penetration of rack profiles in the piece. The calibration area of racks, length Lc, constant height profile, has to be bigger than $\pi d_0/2$, thus ensuring uniform height of processed profile throughout the circumference of the piece.
The deformation process starts at the contact of the semi product of diameter d_0 with the rack slope, fig. 2. Since it works with two racks, on the angle of rotation of the piece 0-π, the rack enters the piece radially, starting from 0 to maximum value g_0:

$$g_0 = \frac{\pi d_0}{2} \cdot P \qquad (1)$$

where: P is the rack slope expressed in mm/100mm and d_0 – diameter of semi product.
For larger angles of rotation of the piece, over π, thickness g_0 of deformed material remains constant until it enters the calibration area. In the calibration area thickness decreases to zero, on an angle of rotation equal to π. The variation of thickness g of deformed material when moving the rack tool is presented in fig. 3.

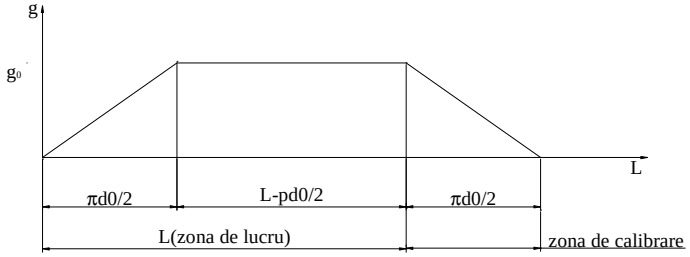

Figure 3. Penetration of the rack into the semi product

When the two racks enter the piece radially, they move volumes of material outward. After the first semi rotation of the piece, volume of material V_1 is transferred towards the forming teeth V_1a, V_1b, fig. 4. At the next semi rotation volume V_2 is transferred, then volume V_3, etc.

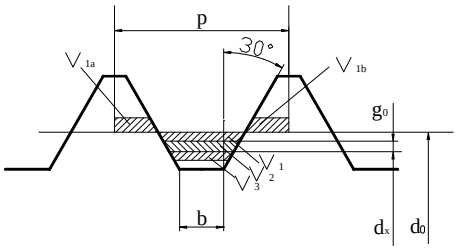

Figure 4. Transfer of the volume of material

The contact between the piece and the rack on the working area, at a certain point, is shown schematically in fig. 5.

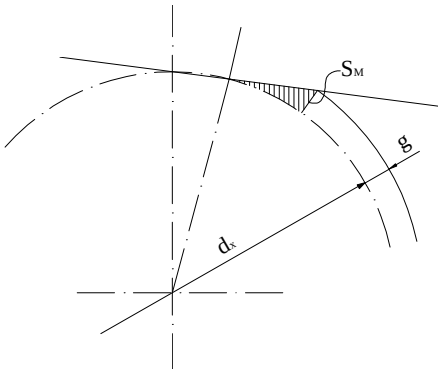

Figure 5. Contact between the piece and the rack

The maximum value of surface S_M, corresponding to volume of material V_1 deformed at the first semi rotation of the piece, is given by relation:

$$S_{M1} = g_0(b+2\cdot h\cdot tg\ \alpha) \quad (2)$$

where b is the peak dimension of rack profile and h is the maximum depth of penetration of the rack tooth in the semi product.
Considering relation (1) we may write:

$$S_{M1} = P\cdot\frac{\pi d_0}{2}(b+2\cdot h\cdot tg\ \alpha) \quad (3)$$

Volume of material V_1 deformed at the first semi rotation of the piece can be expressed as a product between the surface S_{M1} and the contact length between the rack and the semi product, l_c. On the angle of rotation 0-π, the contact length varies from zero to l_c, then for angles larger than π, the contact length l_c remains almost constant, as a result of the fact that g_0 is constant, the following relation is given:

$$l_c = \sqrt{\left(\frac{d_0}{2}\right)^2 - \left(\frac{d_0}{2} - g_0\right)^2} = \sqrt{d_0\cdot g_0 - g_0^2} \cong \sqrt{d_0\cdot g_0} \quad (4)$$

It results that the maximum volume of material V_1 deformed after the rotation of the piece with angle π is approximately given by relation:

$$V_1 = S_{M1}\cdot l_c = P\cdot\frac{\pi d_0}{2}(b+2htg\alpha)\cdot\sqrt{d_0\cdot g_0} \quad (5)$$

Volume of material deformed V_1 determines the maximum forming force at the first semi rotation of the piece; the forming force depends on the same parameters as volume V_1 : slope P of the rack; peak dimension b of the rack tooth; initial diameter d_0 of the piece; expression $2htg\alpha.$, which takes into account the maximum depth of deformation *h* and the slope angle of the rack, α.

At the second semi rotation of the piece, section S_M will decrease, having the expression:

$$S_{M2} = g_0[b+2(h-g_0)\cdot tg\ \alpha] \quad (6)$$

At the third semi rotation, section S_M is:

$$S_{M3}=g_0[b+2(h-2g_0)\cdot tg\ \alpha] \quad (7)$$

It results that when the rack moves along its length, the forming force has an evolution similar to that presented graphically in fig.6.

This evolution does not take into account the fact that at semi rotations 2, 3 and the following, the contact surface between the piece and the rack on a tooth increases and at the end of the rack slope it is maximal. This makes the evolution of force to be slightly modified; an increase of force appears at the end of the penetration in the piece.

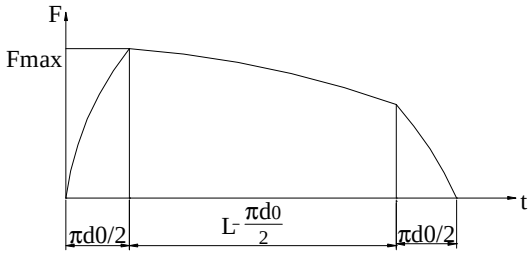

Figure 6. Evolution of the forming force

The deformation force can be assessed by its radial component, Fr, considering that its second component, the tangential one, has very low values in comparison to those of the radial force.

THE MODELS ADOPTED AND THE EXPERIENCE PLAN USED

Three models were taken into account to determine the main component of the deformation force, radial force Fr.

The first model takes into account the depth of profile, h, the rack slope, P, and the material processed through its hardness HB, and has the form:

$$F_r = a_0 \cdot h^{a_1} \cdot P^{a_2} \cdot HB^{a_3} \quad (8)$$

The second model takes into account, in addition to the first, the angle of inclination α of the processed profile flank:

$$F_r = a_0 \cdot h^{a_1} \cdot P^{a_2} \cdot HB^{a_3} \cdot \alpha^{a_4} \quad (9)$$

In addition to the second model, the third one takes into account dimension *b* from the peak of rack profile and the penetration depth *h* is corrected based on the angle of inclination of profile flank:

$$F_r = a_0 \cdot (2\cdot h\cdot tg\alpha)^{a_1} \cdot P^{a_2} \cdot HB^{a_3} \cdot b^{a_4} \quad (10)$$

The natural values of input parameters taken into account to model the process and varied within the experience plan are presented in table 1.

The experience plans were not orthogonal, due to difficulties in achieving the input parameters at the established values.

The experiments were performed on 4 materials, using two racks with different lengths to obtain different slopes, and the deformation depths were varied in wide ranges. At calculations, there were taken into account the real slopes of racks determined function of the deformation depth and the real length of the rack in the deformation process, knowing the speed of racks and the duration of the rolling process.

The rolling speed was approximately constant. For all experiments it had values between 15.3 and 15.9 m/min.

Table 1. Natural values of independent variables

Varied parameter	Symbol	Natural values			
Depth of penetration in material	h, mm	Specific to each sample, in the range of values (0.283 – 0.789) mm			
Real slope	P, mm/1000 mm	Specific to each sample, in the range of values (0.59 – 2.35) mm (calculated function of the deformation depth and length of the working area)			
		Short rack		Long rack	
		$p = \frac{h}{300} \cdot 1000$		$p = \frac{h}{476} \cdot 1000$	
Hardness of processed material	HB	Specific to the type of material processed			
		OLC 15	OLC 35	18MnCr11	40Cr10
		156.1	177.4	211	277.4
Profile angle	α radians	$\pi/12 = 0.261799$			
Peak size of rack profile	b mm	0.732			

EXPERIMENT STAND

The stand used, fig.7 and 8, is designed and built on a special rolling machine, Roto-Flo model 3225. On wedges 1 and 2 which move in opposite directions there are assembled the two sets of racks: long racks 3 and short racks 4. The inductive displacement transducers WA2 measure the deformations of the system under the action of the radial forming forces. The transducers were connected to the strain bridge, and the bridge to the system acquiring data composed by: SPIDER, a computer and the programme to acquire data CATMAN. The piece to be processed 5 is assembled between peaks 6 and 7 and rotates freely during the rolling process.

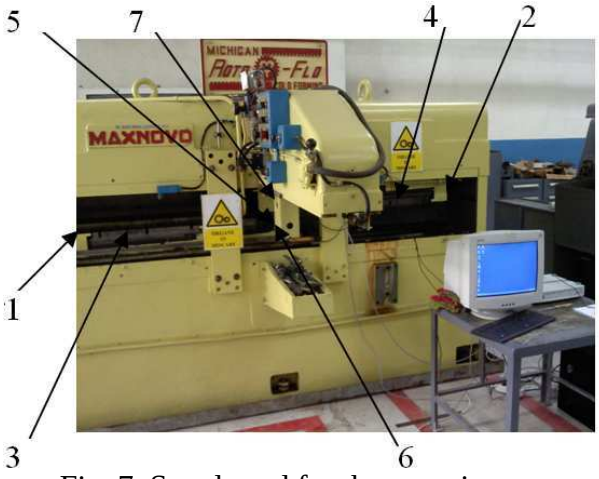

Fig. 7. Stand used for the experiments

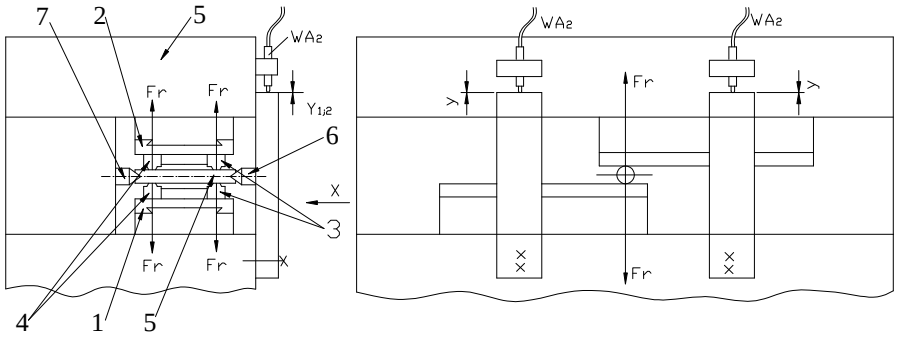

Fig. 8. Scheme to assembly the transducers

The rack tools are made of steel K110 and have values of hardness between 62 and 64 HRC. Five profiles were made on each rack [2]. The values of the slope angles of the two sets of racks are presented in table 2.

Table 2. Values of the rack slopes

Rack	Slope angle, α_0 [°]	Slope mm/mm
Short	0°9'13"	0.8/300
Long	0°5'49"	0.8/476

The semi products were obtained from four types of steel, two types of hardening steels and two types of improving steels: OLC15, OLC35, 18MnCr11, 40Cr10. The mechanical properties of the materials chosen vary in a wide range and are presented in table 3.

Table 3. Mechanical characteristics of materials

Steel mark	Average value calculated using the measured values				Calculated characteristic
	HB [kg/mm^2]	$Rp_{0,2}$ [N/mm^2]	Rm [N/mm^2]	A5 [%]	CMP A5 /HB
OLC 15	156.1	298	475	15	0.10
OLC 35	177.4	248	558	13	0.07
18MnCr11	211	309	776	10	0.05
40Cr10	277.4	396	837	7	0.03

In the case of the experiments the tangential component was also measured indirectly by measuring the pressure in the hydraulic drive motors of the two wedges with transducer P8AP, (Hottinger mark), thus, confirming that its value is very small in comparison to the radial one.

RESULTS OBTAINED

The parameters measured were: tangential speed of racks, pressure in the hydraulic motors and radial forming force. The tangential component of the forming force was determined indirectly through the pressure in the hydraulic motors. The tangential force F_t is small as a result of friction in guides of the wedges, given by the radial force and the force required by the idling of a wedge.

Data recorded during the rolling process were processed in the form of three graphs: cumulative graph, the electrical signals recorded from the transducers measuring the forces, the speed and the pressure; radial force graph; graph of pressure in the hydraulic motor, fig. 9.

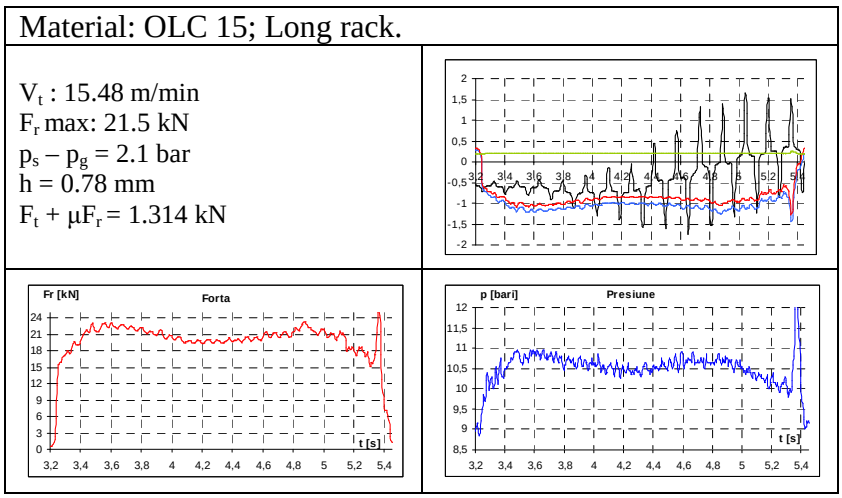

Figure 9. Graphic processing of recorded data

Maximum values of the radial deformation forces are presented in table 4.

The curves of evolution in time of the radial deformation force depending on the process parameters considered, for the entire experience plan, were represented. For example, fig. 10 presents the evolution of force function of the deformation depth for steel OLC15, long rack.

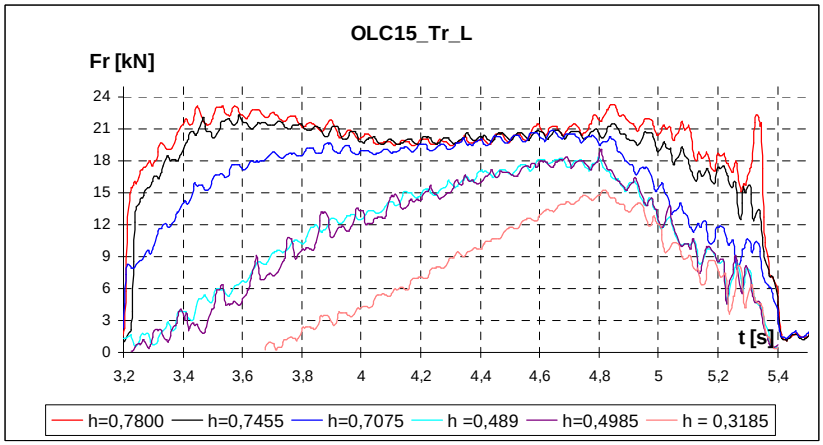

Figure 10. Evolution in time of the forming force for different depths of deformation

Table 4. Values of maximum radial forces for trapezoidal profile

No. exp.	Rack	Material	h [mm]	p	HB	Fr [kN]
1	Short Slope 0.8/300	OLC15	0.2995	0.998333	156.1	16,.56
2			0.487	1.623333	156.1	18.07
3			0.517	1.723333	156.1	18.36
4			0.663	2.21	156.1	20.7
5		OLC35	0.705	2.35	177.4	23.18
6			0.5605	1.868333	177.4	21.26
7			0.509	1.696667	177.4	20.63
8			0.316	1.053333	177.4	17.58
9		18MnCr11	0.6875	2.291667	211	24.84
10			0.522	1.74	211	22.72
11			0.5135	1.711667	211	22.43
12			0.36	1.2	211	20.4
13		40Cr10	0.6895	2.298333	277.4	30.8
14			0.5035	1.678333	277.4	27.31
15			0.32	1.066667	277.4	24.1

16	Long Slope 0.8/476	OLC15	0.7075	1.486345	156.1	20.38
17			0.4985	1.047269	156.1	17.95
18			0.489	1.027311	156.1	17.9
19			0.3185	0.669118	156.1	15
20		OLC35	0.709	1.489496	177.4	22.53
21			0.5025	1.055672	177.4	19.6
22			0.3205	0.673319	177.4	17
23		18MnCr11	0.7065	1.484244	211	24.23
24			0.469	0.985294	211	20.8
25			0.312	0.655462	211	18.5
26		40Cr10	0.682	1.432773	277.4	30.07
27			0.47	0.987395	277.4	26.4
28			0.283	0.594538	277.4	22.7

PROCESSING EXPERIMENTAL DATA

Functions deformation forces, taken as models in relations (8), (9) and (10), are first order polynomial functions, which can be treated by multivariate regression analysis. Using the values of radial deformation forces, obtained experimentally, the constants and exponents of these functions were determined using LINEST application of EXCEL. LINEST uses the method of least squares to calculate the regression line which best describes the data and offers additional regression statistics which certify the adequacy of the model and the fact that independent variables are significant from a statistic point of view. The values obtained for the equation coefficients and exponents of variables, for the three models, are presented in table 5.

Table 5. Constants of functions radial forces of deformation

Model	Function radial force of deformation, F_r [kN]	Constants of function F_r				
		a_0	a_1	a_2	a_3	a_4
1	$F_r = a_0 \cdot h^{a_1} \cdot P^{a_2} \cdot HB^{a_3}$	0.663043	0.247932	0.077416	0.68622	-
2	$F_r = a_0 \cdot h^{a_1} \cdot P^{a_2} \cdot HB^{a_3} \cdot \alpha^{a_4}$	0.250876	0.173489	0.284860	0.728199	-0.478896
3	$F_r = a_0 \cdot (2 \cdot \mathrm{h} \cdot \mathrm{tg}\alpha)^{a_1} \cdot P^{a_2} \cdot HB^{a_3} \cdot b^{a_4}$	0.526424	0.173489	0.284860	0.728199	0.644381

The main statistical regression parameters given by LINEST are presented in table 6.

Table 6. Statistical parameters of regression

Model	Function radial force of deformation F_r [kN]	Statistical parameters of regression				
		Coefficient of determination $R^2 = \frac{SS_A}{SS_A + SS_T}$	Standard deviation of coefficients $s_T = \sqrt{\frac{SS_T}{n-p}}$	Ficher Statistics $F = \frac{\frac{SS_A}{p-1}}{\frac{SS_T}{n-p}}$	Sum of average squared residuals SS_A	Sum of squared residuals SS_T
1	$F_r = a_0 \cdot h^{a_1} \cdot P^{a_2} \cdot HB^{a_3}$	0.986001	0.022319	563.4835	0.842106	0.011956
2	$F_r = a_0 \cdot h^{a_1} \cdot P^{a_2} \cdot HB^{a_3} \cdot \alpha^{a_4}$	0.934766	0.075353	197.0298	4.475004	0.312294
3	$F_r = a_0 \cdot (2 \cdot \mathrm{h} \cdot \mathrm{tg}\alpha)^{a_1} \cdot P^{a_2} \cdot HB^{a_3} \cdot b^{a_4}$	0.934766	0.075353	197.0298	4.475004	0.312294

Within the experiments performed, each independent variable has a certain range of variation and different natural values expressed in different units of measurement.
In order to be able to correctly interpret the results obtained and assess the significance of each process parameter, the regression line equation obtained based on experimental results has to be expressed function of standard variables z_i, varied on two levels, -1 and +1
The general equation of the regression line in standard variables has the form:

$$Y = B_0 + \sum_{i=1}^{n} B_i \cdot z_i \tag{11}$$

where the standard variables z_i are calculated with the following change of variable relation:

$$z_i = \frac{2X_i - (X_{i\max} + X_{i\min})}{X_{i\max} - X_{i\min}} \tag{12}$$

where X_i are standard variables of the regression line and $X_{i\,min}...X_{i\,max}$ is their variation range.
Coefficients B_i are significant for a set level of confidence if their value is higher than their variation range, namely:

$$|B_i| \geq \Delta B_i \text{, where } \Delta B_i = \pm t \cdot s_{B_i} \tag{13}$$

where variable t is quantile to Student distribution.
Standard deviation of coefficients, s_{B_i}, is calculated function of total dispersion s_T^2 with relations:

$$s_{B_0}^2 = \frac{s_T^2}{n} \text{ and } s_{B_i}^2 = \frac{s_T^2}{\sum z_i^2} \tag{14}$$

Values of coefficients B_0 and B_i, for all three models of functions – radial deformation force – are presented in table 7.

Table 7. Regression lines coefficients in standard variables

Model	General equation of regression line in standard variables	B_0	B_1	B_2	B_3	B_4
1	$Y = B_0 + \sum_{i=1}^{n} B_i \cdot z_i$	3.065943	0.113852	0.053199	0.197276	-
2		2.888457	0.079667	0.195754	0.209344	0.165973
3		2.890578	0.120710	0.195754	0.209344	0.12281

The influence of independent variable X_i on dependent variable Y can be assessed based on indicators q_i or q_i %, defined by the absolute or relative variation of variable Y corresponding to variation $X_{i\,min}...X_{i\,max}$ of variable X.

$$q_i = \frac{Y_{\max}}{Y_{\min}} \text{ and } q_i\% = \frac{Y_{\max} - Y_{\min}}{Y_{\min}} \cdot 100\,\% \tag{15}$$

where $Y_{min}...Y_{max} = Y(X_{min}\ldots X_{max})$, for set values of the other variables.
The absolute q_i and relative q_i% weight coefficients were calculated starting from the regression lines equation in standard variables, for all three models; the values obtained are presented in table 8.

Table 8. Values of weight coefficients

Model 1 $F_r = a_0 \cdot h^{a_1} \cdot P^{a_2} \cdot HB^{a_3}$			
Independent variable	Variation mode of the force when increasing the value of independent variable	Dependent variable: force Fr [kN]	
		Absolute weight coefficient, q_i	Relative weight coefficient, q_i%
Deformation depth, h	Increasing	1.26	25.57
Rack slope, P	Increasing	1.11	11.23
HB hardness of material	Increasing	1.48	48.37
Model 2 $F_r = a_0 \cdot h^{a_1} \cdot P^{a_2} \cdot HB^{a_3} \cdot \alpha^{a_4}$			
Deformation depth, h	Increasing	1.17	17.27
Rack slope, P	Increasing	1.47	47.92
HB hardness of material	Increasing	1.52	51.99
Profile angle α	Decreasing	1.39	39.36
Model 2 $F_r = a_0 \cdot (2 \cdot h \cdot tg\alpha)^{a_1} \cdot P^{a_2} \cdot HB^{a_3} \cdot b^{a_4}$			
Deformation depth, h	Increasing	1.27	27.30
Rack slope, P	Increasing	1.48	47.92
HB hardness of material	Increasing	1.52	51.99
Peak size of profile, b	Increasing	1.39	39.36

CONCLUSIONS

The evolution in time of forces recorded confirms the predictions of the theoretical study. Some differences recorded during the experiments are generated by clearances in the guides of rack wedges.

Three models of machinability functions were determined using the values of radial deformation forces obtained after applying the experience plan established.

The regression analysis proved that all models are adequate and have a determination coefficient between 0.93 and 0.98. The most precise model is the first because it does not take into account the geometrical elements of the profile. In the other two models, the profile parameters appear as independent variables, but since the other parameters have the same values there are no significant differences.

The analysis of the influence of process parameters on the radial deformation forces through the values of weight coefficients points out the following elements:

- The hardness of material to be processed has a significant influence on the deformation force: an increase of HB hardness from minimum value of 156.1 units to maximum value of 277.4 units determines an increase of the deformation force with 48.37% - for the first model and with 51.99% - for the second and third models. It results that hardening steels are processed with lower deformation forces than improving steels and the presence of chrome between the alloying elements leads to an increase of the deformation force.
- The influence of the rack slope on the working area is equally important. In the case of the first model, the increase of the value of the rack slope between the range 0.594538 – 2.35 leads to an increase of the radial force with 11.23%. For the other two models, the increase of the slope leads to an increase of the deformation force with 47.92%, hence the strong influence of profile geometry on the deformation force. Lower deformation forces are

obtained when processing with long racks and slopes smaller than those of short racks, the material is deformed gradually, in several stages.

- A much smaller increase of the radial force is determined by the increase of the deformation depth from the minimum value of 0.283 mm to the maximum value of 0.789 mm, namely: 27.3% for model 3, 17.27% for model 2 and 12% for the first model. Generally, minimum deformation forces correspond to small depths of penetration. The correction of the depth of deformation is justified considering the profile angle, which led, in the case of model 3, to limiting the increase of deformation force on the range of variation of penetration depth.
- The relative weight coefficient corresponding to the peak dimension of profile, for model 3, is significant (39.36%), which explains why the parameter is considered an independent variable.
- The third model is more balanced from the point of view of the influence of parameters on the force. By using another experience plan, this third model could be developed to five variables: penetration depth h, rack slope P; hardness of processed material HB; peak dimension of rack profile b and profile angle α.

ACKNOWLEDGEMENTS

This work was supported by CNCSIS – UEFISCDI, project number PN II - IDEI 711/2008 and the project "Supporting young PhD students with frequency by providing doctoral fellowships", co-financed from the EUROPEAN SOCIAL FUND through the Sectoral Operational Program Development of Human Resources.[3]

REFERENCES

1. Iacomi, D., Cercetări privind prelucrările prin D.P.R. a danturilor la piese cilindrice cu scule cremalieră, Teză de doctorat, Universitatea Politehnică din Bucureşti, 1998.
2. Iacomi, D., Ungureanu, I., Niţu, E., Iordache, M., Tudor, M., Experimental study of forming forces on flat wedge tools profiles rolling, International Conference on Manufactoring Science end Education – MSE 2011, 4-6th May, Sibiu, 2011.
3. Niţu, E., Ungureanu, I., Iacomi, D., Tabacu, Şt., Iordache, M., Marincei, L., Standuri pentru cercetarea experimentală a proceselor de deformare la rece a profilelor complexe, Raport de cercetare pe 2009 – Proiect PN II IDEI 711/2008, Piteşti, 2009.
4. Niţu, E., Ungureanu, I., Iacomi, D., Tabacu, Şt., Iordache, M., Marincei, L., Cercetări privind modelarea analitică şi numerică a proceselor de deformare plastică volumică la rece a profilelor, Raport de cercetare pe 2010 – Proiect PN II IDEI 711/2008, Piteşti, 2010
5. Tudor, M., Ungureanu, I., Nitu, E., Iordache, M., Iacomi, D., Numerical modelling of the process of cold plastic deformation with tool rack of the profiles, Scientific Buletin Automotive series, year XV, No. 20, vol. A, pp. 25-32, Pitesti, 2010.
6. Wong, C., Lin, J., Dean, T., Effects of roller path and geometry on the flow forming of solid cylindrical components, Journal of Materials Processing Technology, vol. 167, pp. 344-353, 2005.